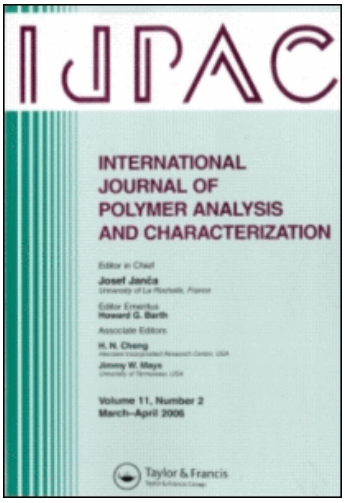

International Journal of Polymer Analysis and Characterization
Publication details, including instructions for authors and subscription information:
http://www.informaworld.com/smpp/title~content=t713646643

Characterization of Semiflexible Polyelectrolyte Solutions in the Presence of Excess Salt: From Dilute to Semidilute Regime

E. Buhler[a]; O. Guetta[a]; M. Rinaudo[a]
[a] Centre de Recherche sur les Macromolécules Végétales (CNRS), Université Joseph Fourier de Grenoble, Grenoble Cedex, France

To cite this Article Buhler, E. , Guetta, O. and Rinaudo, M.(2000) 'Characterization of Semiflexible Polyelectrolyte Solutions in the Presence of Excess Salt: From Dilute to Semidilute Regime', International Journal of Polymer Analysis and Characterization, 6: 1, 155 — 175
To link to this Article: DOI: 10.1080/10236660008034656
URL: http://dx.doi.org/10.1080/10236660008034656

Int. J. Polym. Anal. Charact.,
2000 Vol. 6, pp. 155–175
Reprints available directly from the publisher
Photocopying permitted by license only

Characterization of Semiflexible Polyelectrolyte Solutions in the Presence of Excess Salt: From Dilute to Semidilute Regime*

E. BUHLER†, O. GUETTA and M. RINAUDO

Centre de Recherche sur les Macromolécules Végétales (CNRS), Université Joseph Fourier de Grenoble, BP 53, 38041 Grenoble Cedex, France

(Received 7 December 1999; In final form 19 January 2000)

Highly charged semiflexible polyelectrolyte chitosan was characterized in dilute and semidilute aqueous solutions in the presence of excess of salt by viscosity and static and dynamic light scattering. In the present paper, we report on the variation of the structural and dynamical parameters as a function of the ionic strength. Size of the polyions, virial coefficients and overlap concentration are parameters that are strongly influenced by excess salt concentration.

Keywords: Polyelectrolyte; Semiflexible chains; Chitosan; Static and dynamic light scattering; Intrinsic viscosity

INTRODUCTION

Chitin and chitosan are important polysaccharides extracted from different sources (crabs or shrimp shells, *etc.*). These polymers are composed of $\beta 1 \rightarrow 4$ D-glucosamine units with a variable degree of *N*-acetylation. When the average degree of *N*-acetylation is lower than approximately 0.5, the polymers are called chitosans and they become soluble in aqueous solutions in the presence of acids.[1]

* Presented at the 12th International Symposium on Polymer Analysis and Characterization (ISPAC-12), La Rochelle, France, June 28–30, 1999.

† Corresponding author.

An essential parameter concerning the solutions of linear polymers is the polymer chain rigidity which is strongly influenced by the ionic strength and, in particular, by the polymer concentration in the case of polyelectrolytes. Electrostatic repulsions between the charges along the chain will affect the local flexibility of the chain and will tend to increase the global size of the polyion. For polyelectrolytes, the total persistence length L_p is written as [2]

$$L_p = L_0 + L_e \tag{1}$$

The total persistence length represents the effective rigidity of the polyelectrolyte as the sum of two contributions: the intrinsic persistence length L_0 due to the rigidity of the corresponding uncharged chain and the electrostatic persistence length L_e arising from the repulsion between ionic sites. The value of the intrinsic persistence length of chitosan is estimated between 50 and 150 Å; [1] the rigidity of this polymer is quite important even in high-ionic strength solutions. For polysaccharides, the electrostatic contribution L_e is smaller than the intrinsic contribution L_0. This is the reason why chitosan and polysaccharides in general, are called semirigid or rigid polymers. Several workers [2–5] have calculated the electrostatic contribution to the persistence length L_e. By assuming a Debye–Hückel potential and under condition that the condensation model applies, [6] Odijk [2] and Skolnick and Fixman [3] have derived a formula giving L_e

$$L_e = \frac{1}{4\kappa^2 l_B} \quad \text{for } \lambda_0 > 1 \tag{2}$$

where l_B is the Bjerrum length ($l_B = e^2/\varepsilon_0 kT = 7.13$ Å in water, ε_0 is the dielectric permittivity of the solvent, and e the elementary charge) and κ^{-1} is the Debye–Hückel screening length related to the concentration of the counter ions. The structural charge parameter was $\lambda_0 = 1.24$ in our case [1] ($\lambda_0 = e^2/\varepsilon_0 kTa$, a being the distance between two ionic sites). In dilute polyelectrolyte solutions, in the presence of excess of salt of the concentration c_s

$$\kappa^2 = 8\pi l_B c_s \tag{3}$$

Equation (2) is valid if $\kappa L_P \gg 1$, which is true for polyelectrolytes near the rod limit or at least for polyelectrolytes having a high intrinsic

stiffness. Chitosan having a larger intrinsic persistence length L_0 than the electrostatic persistence length L_e (at least for external salt concentration larger than 3×10^{-3} M), is characterized by high rigidity, even in high ionic strength solutions (κ^{-1} small).

In the present paper, we report the results of viscosity and light scattering experiments performed on 0.3 M acetic acid solutions of a 190000 g/mol semiflexible polyelectrolyte chitosan for polymer concentrations ranging from 10^{-4} to 4×10^{-3} g/cm^3, for excess salt concentrations (sodium acetate) ranging from 0.05 to 0.2 M and at a temperature 25°C. Typical "good solvent" behavior is found. Viscosity and light scattering measurements were carried out to determine structural and dynamical parameters as a function of the ionic strength. Size of polyions, virial coefficients and crossover concentration between the dilute and semidilute regimes are parameters that are strongly influenced by the excess of salt concentration.

MATERIALS AND METHODS

Sample Characteristics

We have investigated solutions of 190000 g/mol polysaccharide chitosan, which is a semirigid polyelectrolyte from PROTAN composed of β 1→4 D-glucosamine units with a degree of *N*-acetylation equal to 12%. The polysaccharide chitosan belongs to a family of linear cationic biopolymers obtained from alkaline *N*-deacetylation of chitin, which is the second most abundant polymer in nature. The polydispersity $M_w/M_n = 1.3$ was determined by GPC, where M_w is the weight-average molecular weight and M_n the number-average molecular weight.[1] The contour length is equal to $L_c = 6000$ Å. In acid conditions, chitosan is water-soluble due to the presence of protonated amino groups and it exhibits a polyelectrolyte character. The solutions were investigated in the polymer concentration range from 1×10^{-4} to 4×10^{-3} g/cm^3 at 25°C and in 0.3 M acetic acid in the presence of sodium acetate. The concentration of sodium acetate (excess of salt) varied between 0.05 and 0.2 M. For 0.3 M in acetic acid, all the amino groups are protonated and chitosan exhibits a polyelectrolyte character.[1]

To carry out the static and dynamic light scattering experiments, all solutions were filtered directly into the light scattering cells through 0.1 μm or 0.2 μm Sartorius cellulose nitrate membranes. The solutions were filtered also before viscosity measurements. No aging effects were observed.

Viscosity Measurements

The viscosity measurements were carried out by using a low-shear 30 coaxial viscometer, on the Newtonian plateau, within the range of polymer concentration from 10^{-4} to 4×10^{-3} g/cm^3, which is the same as for the light scattering experiments.

Static Light Scattering

Static light scattering (SLS) and dynamic light scattering (DLS) experiments were performed by means of a spectrometer equipped with an argon-ion laser (Spectra Physics model 2020) operating at $\lambda = 488$ nm, an ALV-5000 correlator (ALV, Langen-Germany Instruments) a computer-controlled and stepping-motor-driven variable angle detection system, and a temperature-controlled sample cell. Temperature was 25 ± 0.1°C unless otherwise noted. The scattering spectrum was measured through a band-pass filter (488 nm) and a pinhole (200 μm for the static experiments and 100 or 50 μm for the dynamic experiments) with a photomultiplier tube (ALV).

In the SLS experiments, the excess scattered intensity $I(q)$ was measured with respect to the solvent, where the magnitude of the scattering wave vector q is given by

$$q = \frac{4\pi n}{\lambda} \sin \frac{\theta}{2} \tag{4}$$

In Eq. (4), n is the refractive index of the solvent (1.34 for the water at 25°C), λ is the wavelength of light in the vacuum, and θ is the scattering angle. In our experiments, the scattering angle θ was varied between 20° and 150°, which corresponds to scattering wave vectors q in the range from 6×10^{-4} to 3.2×10^{-3} Å^{-1}. The absolute scattering intensities $I(q)$ (*i.e.*, the excess Rayleigh ratio) were deduced by using a

toluene sample reference for which the excess Rayleigh ratio is well known.

A virial expression for the osmotic pressure can be used in dilute regime to deduce the following relationship:

$$\frac{Kc}{I(q,c)} = \frac{1}{M_w}\left[1 + q^2\frac{R_G^2}{3} + \cdots\right] + 2A_2Q(q,c)c + \cdots \tag{5}$$

The function $Q(q,c)$ is approximately unity for flexible polymer chains, but not for spheres,[7] $Q(0,c)$ is equal to 1 in any case. c is the polymer concentration and A_2 is the second virial coefficient, which describes the polymer-solvent interactions. The scattering constant is $K = 4\pi^2 n^2 (dn/dc)^2 / N_A \lambda^4$ where dn/dc is the refractive index increment and N_A is Avogadro's number. The dn/dc of the polysaccharide chitosan in the solvent composed of 0.3 M acetic acid + sodium acetate is equal to 0.195.[1] The plots of $c/I(q,c)$ *versus* q^2 were extrapolated to $q=0$ to give intercepts $c/I(0,c)$. For infinite dilute solutions, the average radius of gyration R_G can be determined from the intercept and the initial slope of these plots using a scattering inverse Lorentzian law of the form[7]

$$\frac{c}{I(q,c)} = \frac{c}{I(0,0)}\left[1 + \frac{q^2R_G^2}{3}\right] \quad \text{with } c \to 0 \tag{6}$$

The weight-average molecular weight[7] M_w can be obtained from

$$\frac{Kc}{I(0,c)} = \frac{1}{M_w} + 2A_2c \tag{7}$$

Dynamic Light Scattering

In the dynamic light scattering experiments (DLS), the normalized time autocorrelation function $g^{(2)}(q,t)$ of the scattered intensity is measured.[7]

$$g^{(2)}(q,t) = \frac{\langle I^*(q,0)I(q,t)\rangle}{\langle I(q,0)\rangle^2} \tag{8}$$

The latter can be expressed in terms of the field autocorrelation function or equivalently in terms of the autocorrelation function of the

concentration fluctuations $g^{(1)}(q, t)$ through

$$g^{(2)}(q, t) = A + \beta|g^{(1)}(q, t)|^2 \tag{9}$$

where A is the baseline and β is the coherence factor which in our experiments is equal to 0.7–0.9. The normalized dynamical correlation function $g^{(1)}(q, t)$ of polymer concentration fluctuations is defined as

$$g^{(1)}(q, t) = \frac{\langle \delta c^*(q, 0)\delta c(q, t)\rangle}{\langle \delta c(q, 0)^2\rangle} \tag{10}$$

where $\delta c(q, t)$ and $\delta c(q, 0)$ represent fluctuations of polymer concentration at time t and zero, respectively.

In our experiments, the inspection of the angular dependence shows that the relaxation in dilute and semidilute regimes is diffusive with characteristic times inversely proportional to q^2. Consequently, we have adopted the classical cumulant analysis.[8] This analysis provides the variance of the correlation function and the first reduced cumulant $(\tau q^2)^{-1}$ where τ is the average relaxation time of $g^{(1)}(q, t)$. The extrapolation of $(\tau q^2)^{-1}$ to $q = 0$ yields the values of the mutual diffusion constant D. The latter is related to the average hydrodynamic radius R_H of the macromolecules through

$$D = \frac{kT}{6\pi\eta_s R_H} = \left(\frac{1}{\tau q^2}\right)_{q^2=0} \tag{11}$$

where k is the Boltzman constant, η_s the solvent viscosity and T the absolute temperature.

Figure 1 shows the semilog plot of $g^{(1)}(q, t)$ for a solution of chitosan at a polymer concentration of 3×10^{-4} g/cm^3 in the solvent composed of 0.3 M acetic acid + 0.05 M sodium acetate and at 25°C. The scattering angle θ is equal to 90°.

Another method to determine the average relaxation time τ is the Contin method based on the inverse Laplace transform of $g^{(1)}(q, t)$.[9] If the spectral profile of the scattered light can be described by a multi-Lorentzian curve, then $g^{(1)}(q, t)$ can be written as

$$g^{(1)}(q, t) = \int_0^\infty G(\Gamma)\exp(-\Gamma t)d\Gamma \tag{12}$$

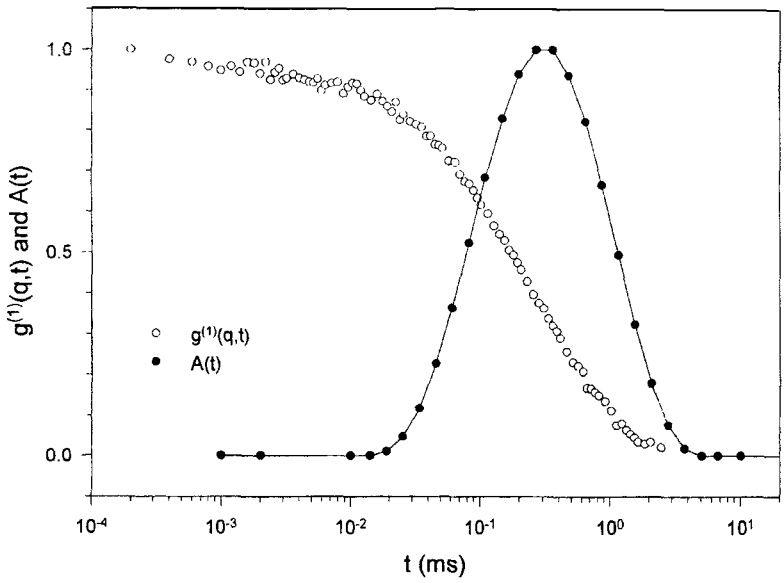

FIGURE 1 Semilog representation of $g^{(1)}(q,t)$ for $\theta = 90°$ relative to 0.3 M acetic acid + 0.05 M sodium acetate solutions of chitosan at 25°C and at polymer concentration 3×10^{-4} g/cm^3 (○). The normalized distribution function of decay times $A(t)$ obtained using the Contin method (●).

where $G(\Gamma)$ is the normalized decay constant distribution. This method is more appropriate for solutions characterized by several relaxations mechanisms (*e.g.*, mixture of polymers and aggregates). We also used the Contin method.[9] Figure 1 shows a typical example of results obtained by applying the Contin method to our data for a dilute solution. $A(t)$ is the normalized distribution function of decay times obtained by using the Contin method. The relaxation times obtained from Contin method coincide quite well with the relaxation times obtained from the cumulant method described earlier.

RESULTS AND DISCUSSION

Viscosity Measurements

In Figure 2, the variation of the specific viscosity $\eta_{sp} = \eta - \eta_s/\eta_s$ with $c[\eta]$ is plotted as a semilog plot for an excess of salt concentration

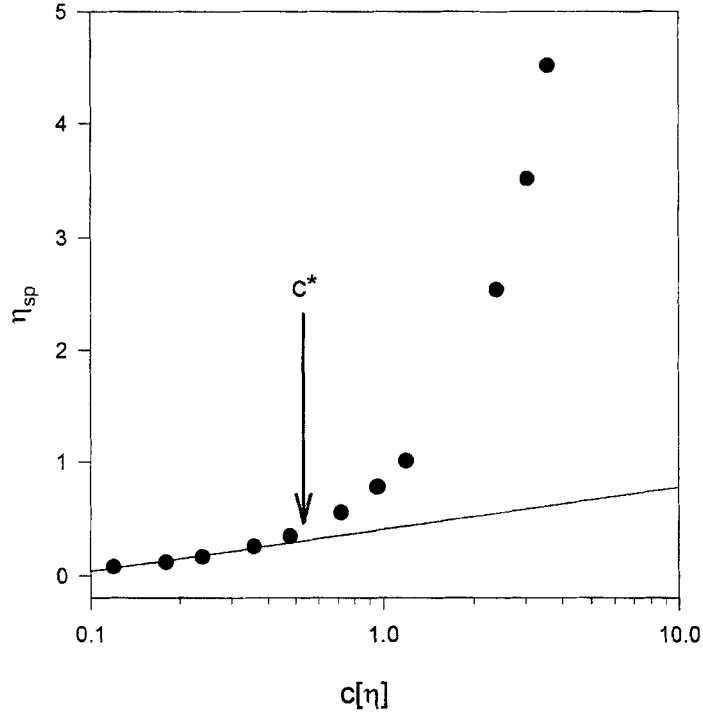

FIGURE 2 Variation of the specific viscosity with $c[\eta]$ for external salt concentration equal to 0.05 M. The line represents a linear best fit of the data in the dilute regime. Deviation from this line (*i.e.*, departure from the Huggins behavior) occurs at the overlap concentration c^*. The arrow indicates the overlap concentration c^*.

equal to 0.05 M. η is the solution viscosity and η_s the solvent viscosity. $[\eta]=\eta-\eta_s/\eta_s c$ (for $c=0$) is the intrinsic viscosity of the solution. The viscosity in the presence of excess salt (acetic acid 0.3 M/ sodium acetate) varies in the Newtonian regime as $\eta_{sp}=c[\eta]+k_H c^2[\eta]^2+Bc^n[\eta]^n$. In the dilute regime, deviation from Newtonian behavior was never observed. B and n are constants introduced to represent all contributions corresponding to an exponent larger than 2. The first two terms correspond to the dilute regime described by the Huggins relation. The Huggins constant k_H was determined for the three studied ionic strengths and from the departure from Huggins behavior we deduced the overlap concentration c^*. Values of $[\eta]$, k_H and c^* for the three studied excess salt concentrations are collected in Table I. Separation between dilute virial regime and overlapped regime is

TABLE I Variation of the Huggins constant k_H, intrinsic viscosity $[\eta]$, $1/[\eta]$, and the overlap concentration c^* deduced from departure from Huggins behavior (see Fig. 2) as a function of excess salt concentration (sodium acetate) for 0.3 M acetic acid solutions of chitosan at 25°C

$[CH_3COONa]$ (M)	k_H	$[\eta]$ (cm^3/g)	$1/[\eta]$ (g/cm^3)	c^* (g/cm^3)
0.05	0.37 ± 0.10	1200 ± 300	$(8.3 \pm 2.0) \times 10^{-4}$	$(5.5 \pm 0.5) \times 10^{-4}$
0.1	0.30 ± 0.10	1100 ± 300	$(9.1 \pm 2.0) \times 10^{-4}$	$(7.5 \pm 0.5) \times 10^{-4}$
0.2	0.30 ± 0.10	900 ± 200	$(1.1 \pm 0.3) \times 10^{-3}$	$(9.0 \pm 1.0) \times 10^{-4}$

characterized by the overlap concentration c^*, *i.e.*, when $c[\eta]$ is about unity.[10]

$$[\eta] = \frac{N_A 4\pi R_\eta^3}{3M} \approx \frac{1}{c^*} \tag{13}$$

where R_η is the hydrodynamic radius and M the molar mass of the polymer chain. According to Eq. (13), the inverse of the intrinsic viscosity can be used to obtain a value of the cross-over concentration separating dilute and semidilute regime (*i.e.*, $c^*[\eta]$ is about unity). To deduce values of c^* we have used the graphical method described earlier (*i.e.*, c^* is the concentration where departure from Huggins behavior occurs (see Fig. 2)), this method being more precise. Values of $1/[\eta]$ are also given in Table I.

The Huggins constant k_H (dimensionless) is usually referred to as the interaction constant[11] and may be viewed as reflecting the combined liquid dynamic and chemical interaction. The k_H values are in agreement with that of neutral polymers ($0.3 < k_H < 0.5$). The variation of k_H with excess salt concentration being small and the error bar of k_H being high, it is difficult to discuss the ionic strength dependence of the Huggins constant k_H. The low value indicates that the long-distance electrostatic interactions are probably almost screened in the three conditions tested.

Static Light Scattering in Dilute Regime

The Zimm plot is a classical graphical technique for simultaneous extrapolation of the light scattering data in the dilute regime to both zero angle and zero concentration. It is constructed by plotting $Kc/I(q,c)$ as a function of q^2+10c, as shown in Figure 3, where K is the scattering constant (see Eq. (5)) and the factor 10 is the chosen constant to give a convenient spacing of the data points on the graph. The concentrations used for the Zimm plot are in the dilute regime and are respectively equal to $c = 10^{-4}, 2\times10^{-4}, 3\times10^{-4}$ and 4×10^{-4} g/cm^3. The solvent is (0.3 M acetic acid + 0.05 M sodium acetate) at 25°C. The data points on the grid corresponding to a given angle are then extrapolated to zero concentration and, similarly, the points at a given concentration are extrapolated to zero angle. The inverse of the

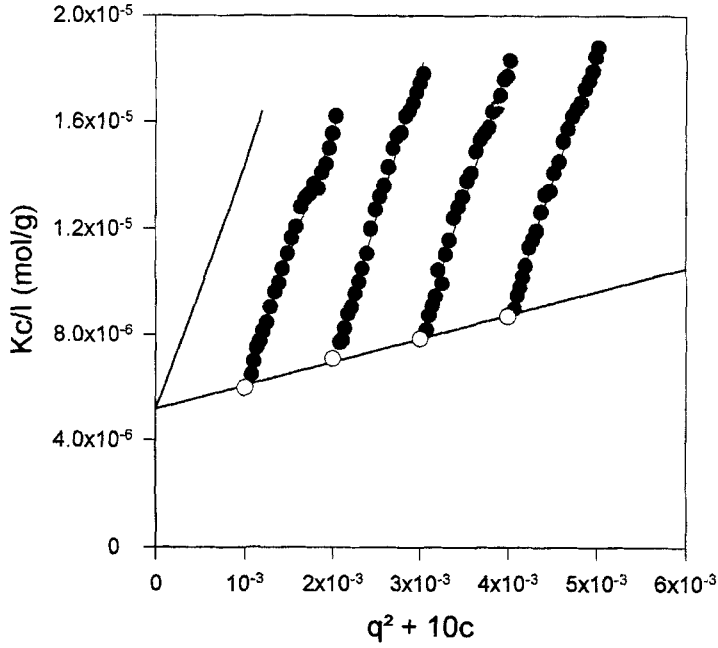

FIGURE 3 Zimm plot of chitosan at 25°C. The solvent is 0.3 M acetic acid + 0.05 M sodium acetate. Points (○) are extrapolation to zero-wave vector and solid lines represent best fits.

weight-average molecular weight M_w is obtained from the intercept of the $q^2 = 0$ curve and the second virial coefficient, A_2, is obtained from the slope ($2A_2 =$ slope). The intercept of the $c = 0$ curve again gives the inverse of the molecular weight, and the initial slope is proportional to the radius of gyration.

The weight-average molecular weight and the radius of gyration found were 195000 ± 5000 g/mol and 70 ± 5 nm, respectively. This value is in good agreement with the commercial one. The value of the radius of gyration is relatively high, thus characterizing a semirigid polymer. The ratio of the hydrodynamic radius (48 nm) and the radius of gyration is equal to 0.68 (see the following section and Table IV for the determination of the hydrodynamic radius). This ratio is equal to 0.8 for flexible monodisperse Gaussian chains [12] in a theta solvent. The polydispersity of our polymer is equal to 1.3 and the solvent is good. For polydisperse, flexible chains in a good solvent, this ratio can be as low as 0.54. [13]

TABLE II Variation of the second virial coefficient A_2, the radius of gyration R_G, and the overlap concentration c^* calculated using Eq. (14) as a function of excess salt concentration (sodium acetate) for 0.3 M acetic acid solutions of chitosan at 25°C

$[CH_3COONa]$ (M)	A_2 $(cm^3 \cdot g^{-2} \cdot mol)$	R_G (nm)	c^* (g/cm^3)
0.05	$(4.47 \pm 0.50) \times 10^{-3}$	70 ± 5	$(2.30 \pm 0.60) \times 10^{-4}$
0.1	$(2.70 \pm 0.20) \times 10^{-3}$	54 ± 5	$(5.0 \pm 1.5) \times 10^{-4}$
0.2	$(1.10 \pm 0.10) \times 10^{-3}$	42 ± 5	$(1.04 \pm 0.30) \times 10^{-3}$

The positive sign of the second virial coefficient, $4.47 \pm 0.50 \times 10^{-3} cm^3 \cdot g^{-2} \cdot mol$, indicates that the 0.3 M acetic acid/ 0.05 M sodium acetate medium is a good solvent for chitosan. The value of the second virial coefficient increases with decreasing excess salt concentration (see Tab. II). A similar trend in the dependence of the second virial coefficient of polyelectrolytes on the salt concentration was observed in previous scattering experiments.[14] The increase of the second virial coefficient is characteristic of the increase of the expansion of the polyelectrolyte chain and electrostatic repulsion interaction. We will see in the following section that the behavior of the second dynamic virial coefficient k_D with excess salt concentration is similar. Values of R_G and A_2 for the three studied salt concentrations are given in Table II.

The overlap concentration c^* can be estimated from the radius of gyration R_G and from the molecular weight M_w obtained from the static experiments. The overlap concentration is assumed to be equal to the density inside the polymer chains.[10]

$$c^* = \frac{3M_w}{N_A 4\pi R_G^3} \tag{14}$$

where N_A is Avogadro's number. Values of c^* deduced from Eq. (14) for the three studied salt concentrations are given in Table II.

Benoît and Doty[15] have used the total persistence length L_p and the total contour length L_c to calculate the unperturbed radius of gyration $\langle R_G^2 \rangle_0$

$$\langle R_G^2 \rangle_0 = \frac{(L_c L_p)}{3} - L_p^2 + \frac{2L_p^3}{L_c} - \frac{2L_p^4}{L_c^2}\left[1 - \exp\left(\frac{-L_c}{L_p}\right)\right] \tag{15}$$

This is the basis of the "wormlike chain" model and serves as a bridge between the rod limit where $L_p \gg L_c$ and $\langle R_G^2 \rangle_0 = L_c^2/12$, and the

random coil limit where $L_c \gg L_p$ and $\langle R_G^2 \rangle_0 = L_c L_p/3$. Equation (15) applies only to semirigid molecules in which there are no excluded volume effects. Excluded volume effects, which modify polymer properties, are based on the interactions between distant segments along a polymer which, *via* chain flexibility, are located in each others' spacial vicinity. Net repulsion among segments (*e.g.*, polyelectrolytes in a "good solvent"), increases the overall dimensions of the polymer. The "perturbed" mean-square-radius of gyration is then $\langle R_G^2 \rangle$ and has often been related to $\langle R_G^2 \rangle_0$ by the static expansion parameter α.[16]

$$\langle R_G^2 \rangle = \alpha^2 \langle R_G^2 \rangle_0 \tag{16}$$

The square expansion coefficient α^2 has been the object of intense theoretical and experimental investigation. We restrict attention to one particular combination of the results introduced in Ref. [17]. The Gupta–Forsman[18] relationship between α and the perturbation parameter z, which has worked well in several cases is, for $N_k \geq 2$,

$$\alpha^5 - \alpha^3 \cong \frac{134}{105}(1 - 0.885 N_k^{-0.462})z \tag{17}$$

where z is given in the long chain limit by[16]

$$z = (3/2\pi L_k^2)^{3/2} \beta N_k^{1/2} \tag{18}$$

L_k and N_k are the length of a Kuhn statistical segment and the number of segments in the polymer, respectively. In the Gaussian coil limit $L_k = 2L_p$. In Eq. (18), β is the excluded volume between two Kuhn segments, which in the case of electrostatic excluded volume measures the electrostatic interactions over all mutual configurations, as suggested by Odijk and Houwaart.[19] Fixman and Skolnick[20] approximated the electrostatic excluded volume between charged rod-like segments of length L_k as

$$\beta = 8L_p^2 \kappa^{-1} \int_0^{\pi/2} \sin^2\theta \int_0^{w/\sin\theta} x^{-1}(1 - \exp(-x))dx d\theta \tag{19}$$

where $w = 2\pi\lambda_0^2 l_B^{-1} \kappa^{-1} \exp(-\kappa d)$, d being the rod diameter.

The static light scattering measures $\langle R_G^2 \rangle$ and not $\langle R_G^2 \rangle_0$, so that L_p cannot be determined directly from the Eq. (15). For electrostatic excluded volume, $\alpha^2 > 1$ at finite salt concentration and L_p contains an

electrostatic contribution; these two values for each ionic concentration can be calculated and compared with the experimental data. We found good agreement between the experimental and the calculated data for an intrinsic persistence length L_0 equal to 70 Å. Table III shows the variation of the calculated radius of gyration, $R_{G,\text{calculated}}$, and of the calculated expansion parameter α with excess salt concentration. Values of L_e and L_p are also given in Table III. The obtained value of 70 Å for L_0 is reasonable and was already proposed in previous studies.[1] Quite low value of α for an excess salt concentration equal to 0.2 M shows that the electrostatic interactions are almost completely screened under such conditions.

Yamakawa[16] used the perturbation theory of excluded volume to express A_2

$$A_2 = (N_A N_k^2 \beta / 2M^2) h_0(z/\alpha^3) \tag{20}$$

with:

$$h_0(z/\alpha^3) = (1 - (1 + 3.9z/\alpha^3)^{-0.468})/(1.83z/\alpha^3) \tag{21}$$

As discussed in Ref. [21, 22] the total A_2 of the polyelectrolyte can be approximated by the sum of A_2. We can define $A_{2,HS}$ the high-ionic

TABLE III Variation of the electrostatic persistence length L_e, total persistence length L_p, the static expansion parameter α, the calculated radius of gyration R_G, and the calculated second virial coefficient A_2 as a function of excess salt concentration. The best agreement with experimental data was found for $L_0 = 70$ Å

$[CH_3COONa]$ (M)	L_e(Å)	L_p(Å)	α	$R_{G,calculated}$ (nm)	$A_{2,calculated}$ $(cm^3 \cdot g^{-2} \cdot mol)$
0.05	6.46	76.46	1.63	61	1.2×10^{-2}
0.1	3.23	73.23	1.48	55	8.1×10^{-3}
0.2	1.62	71.62	1.30	48	5.1×10^{-3}

TABLE IV Variation of the dynamic second virial coefficient k_D, the diffusion coefficient at infinite dilution D_0, the hydrodynamic radius R_H, and the overlap concentration c^* deduced from Figure 5 as a function of the excess salt concentration (sodium acetate) for 0.3 M acetic acid solutions of chitosan at 25°C

$[CH_3COONa]$ (M)	k_D (cm^3/g)	D_0 (nm^2/s)	R_H (nm)	c^* (g/cm^3)
0.05	588 ± 60	$(5.1 \pm 0.5) \times 10^6$	48 ± 4	$(5.5 \pm 0.5) \times 10^{-4}$
0.1	300 ± 30	$(6.5 \pm 0.5) \times 10^6$	38 ± 4	$(6.5 \pm 0.5) \times 10^{-4}$
0.2	37 ± 5	$(8.6 \pm 0.5) \times 10^6$	29 ± 4	$(1 \pm 0.05) \times 10^{-3}$

strength limit of A_2, obtained from experimental extrapolation of A_2 to infinite salt concentration. In this work only three ionic strengths were investigated, so it is difficult to fit the data (A_2 as a function of the external salt concentration c_s) with a power law and to determine $A_{2,HS}$. This treatment was applied with good agreement between experimental and calculated values on hyaluronan.[23] Values of calculated A_2 are given in Table III. Theoretical and experimental values of A_2 are of the same order, even if a shift is observed.

Dynamic Light Scattering

Figure 4, representing the variation of the product $\tau \times q^2$ with q for different polymer solutions shows clearly that the relaxation is a

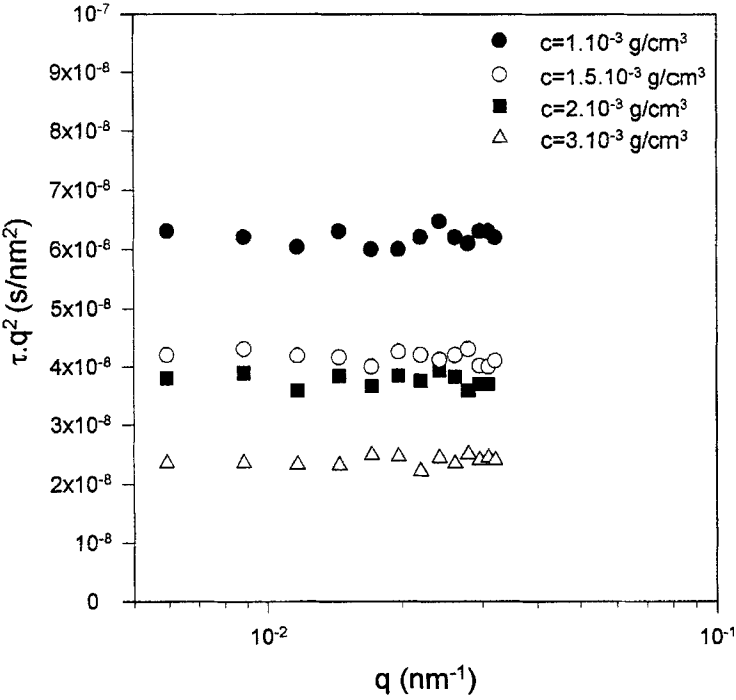

FIGURE 4 Variation of τq^2 with q measured in 0.3 M acetic acid + 0.05 M CH_3COONa sodium acetate solutions with polymer concentration: 1×10^{-3} g/cm^3 (•), 1.5×10^{-3} g/cm^3 (○), 2×10^{-3} g/cm^3 (■) and 3×10^{-3} g/cm^3 (△). Other concentrations are omitted for clarity.

diffusive one with characteristic time τ inversely proportioned to q^2. Thus, it is possible to calculate for each polymer concentration a diffusion coefficient D by using Eq. (11).

The Figure 5 shows the polymer concentration dependence of D for (0.3 M $CH_3COOH + CH_3COONa$) solutions of chitosan at $T = 25°C$. Three excess of salt concentrations (three ionic strengths) were investigated: 0.05 M; 0.1 M and 0.2 M. The diffusion coefficient increases slowly with c at first, then more rapidly as $c[\eta]$ exceeds about unity (see Fig. 2 and Tab. I).

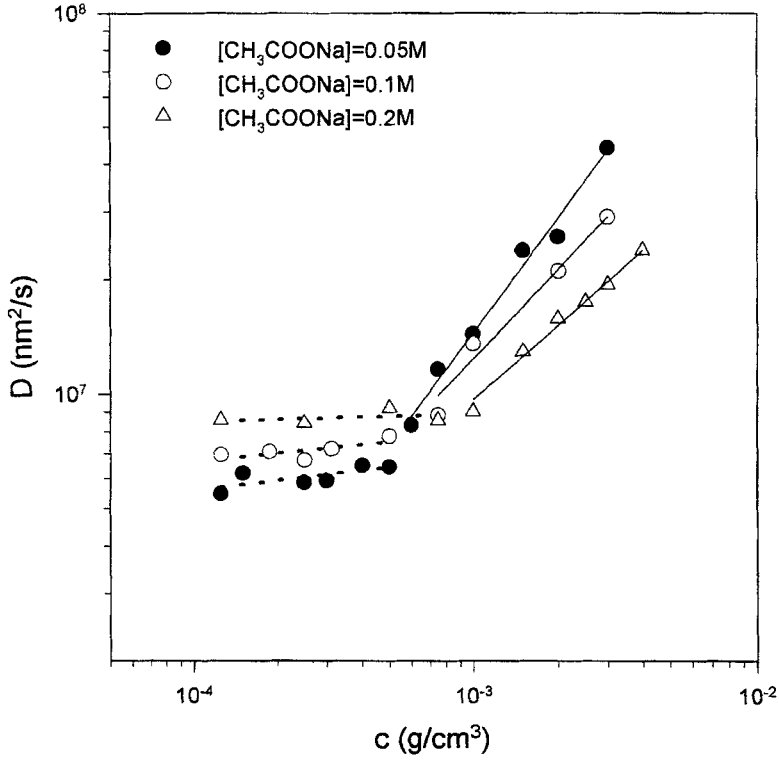

FIGURE 5 Dependence of the diffusion coefficient on the polymer concentration for three excess salt concentrations: 0.05 M (•), 0.1 M (○) and 0.2 M (△). Black lines represent fits of the data in the overlapped regime and dashed lines represent liner-least-squares best fits in the dilute virial regime. The experimental error is equal to 10%.

Dilute Regime

In the dilute polyelectrolyte solution regime, it is observed that the apparent diffusion coefficient D measured is a linear function of the polyelectrolyte concentration

$$D = D_0(1 + k_D c + \cdots) \tag{22}$$

with D the apparent diffusion coefficient, D_0 the apparent diffusion coefficient at infinite dilution, k_D the diffusion second virial coefficient, and c the polyelectrolyte concentration. The separation between the dilute virial regime and the semidilute regime is characterized by the critical overlap concentration c^*. The polyelectrolyte concentration dependence of the apparent diffusion coefficient is linear for all conditions employed (three ionic strengths) and shows that the virial expansion can be limited to the second virial coefficient in the dilute concentration range. The positive sign of k_D indicates that the medium used is a good solvent for chitosan. Figure 5 shows that when decreasing the ionic strength (salt concentration) the polyelectrolyte concentration dependence of the apparent diffusion coefficient becomes stronger. The obtained values for D_0 and k_D with linear-least-squares best fits are given in Table IV. With decreasing ionic strength (salt concentration) D_0 becomes smaller due to the expansion of the polyelectrolyte coil.

Using the Stokes–Einstein equation (see Eq. (11)), we can calculate the hydrodynamic radius R_H using the value of D_0. The values of R_H for the three studied ionic strengths are reported in Table IV. The dependence of k_D on salt concentration is predicted by the small ion-polyion coupled mode theory, as reviewed by Schurr and Schmitz.[24] The molecular theory of Imai and Mandel[25, 26] also predicts this behavior. These authors showed that k_D is proportional to the inverse of the salt excess concentration. The approximate expression[26] obtained for the effective diffusion coefficient up to the linear terms in the polyelectrolyte concentration is

$$\frac{D}{kT} \approx \frac{(M/N_A)(\partial\Pi/kT/\partial c)}{(\omega_p + \omega_s)} \left(1 + \frac{\gamma_p^2 Z^2}{M}\left[1 - \frac{\omega_\pm}{\omega_p + \omega_s}\right]\frac{c}{2c_s} + \cdots\right) \tag{23}$$

with Π the osmotic pressure of the polyelectrolyte solution, M the molar mass of the polyelectrolyte, Z the number of elementary charges on the polyion, c_s the added salt concentration, γ_p the activity coefficient of the counter-ions in the salt-free solution, and ω_p the friction coefficient of the polyelectrolyte. The friction coefficients of the small co-ions and counterions, $\omega_\pm$, are assumed to have identical values. The definition of ω_s is more complicated, but it is proportional to, and of the same order as $\omega_\pm$. The virial expansion for the osmotic pressure is

$$\frac{M\Pi}{N_A kT} = c(1 + A_2 Mc + \cdots) \tag{24}$$

For very dilute solutions, the second virial term can be neglected and then $(M/N_A)\partial(\Pi/kT)/\partial_c$ is about unity. As a result, the second dynamic virial coefficient k_D as defined by Eq. (22) is well approximated by

$$k_D \cong \frac{\gamma_p^2 Z^2}{2Mc_s}\left[1 - \frac{\omega_\pm}{\omega_p + \omega_s}\right] \tag{25}$$

The term between the brackets being about unity[14,26] and the activity coefficient γ_p being ionic strength independent, the Eq. (25) shows that k_D is proportional to the inverse of the excess salt concentration. This k_D dependence with salt concentration was experimentally found by Smits *et al.*[27] and by Tanahatoe *et al.*[14] for linear highly charged polyelectrolyte and is also in a good agreement with our data.

Cross-over Concentration

The overlap concentration can be estimated from Figure 5 (values of c^* are given in Tab. IV). This concentration corresponds to the transition between two regimes observed in the curves characterizing the variation of the diffusion coefficient with the polymer concentration. Cross-over concentrations obtained by using the viscosity and dynamic light scattering data are in very good agreement (see for instance Figs. 2 and 5).

Semidilute Regime

Above the overlap concentration c^*, the diffusion coefficient increases with polymer concentration as shown in Figure 5. In this regime, the variation of the diffusion coefficient with polymer concentration can be described by a power law depending on the ionic strength: $D \approx c^{0.99}$; $D \approx c^{0.78}$ and $D \approx c^{0.65}$ for sodium acetate concentration equal to 0.05, 0.1 and 0.2 M, respectively. The experimental error of the exponent values is equal to 10%.

de Gennes developed a scaling theory for semidilute solutions in thermodynamically good solvents.[10] The main prediction of this theory is that the dynamical behavior of the solution can be described in terms of a single characteristic length that is the correlation length ξ. The cooperative diffusion coefficient D is related with the hydrodynamic correlation length ξ_H that scales like the static correlation length ξ (see Eq. (11)). The correlation length ξ and, consequently, the cooperative diffusion coefficient D follow simple scaling laws with the dilution according to[10]

$$\xi \approx c^{-0.77} \quad \text{and} \quad D \approx c^{0.77} \tag{26}$$

In the semidilute regime, the diffusion coefficient follows a power law which depends on the ionic strength. In the 0.05 M added sodium acetate solution, the diffusion coefficient can be characterized by an exponent equal to 0.99, larger than the theoretical value for neutral polymers in good solvent. For this salt concentration, all charges are not screened even if this salt concentration is not too small compared to 0.1 and 0.2 M. To our knowledge, there is no theoretical model predicting the variation of the diffusion coefficient with polymer concentration for not screened or not totally screened polyelectrolyte solutions. The relaxation corresponds to the contribution of an overlapped solution and the associated fluctuations of concentration relax by a cooperative diffusion mechanism of the meshes of the network, *i.e.*, the correlation length. With the Stoke–Einstein equation (see Eq. (11)), the calculated hydrodynamic correlation length of the semidilute network (ξ_H) ranges between 30 and 7 nm in the investigated concentration range. Consequently, our experiments were carried out in the regime where the mesh size is larger than the persistence length for almost the whole investigated concentration range.

CONCLUSION

This work summarizes viscosity, static and dynamic light scattering results on the dilute and semidilute solution properties of semirigid polyelectrolytes. The data allows us to estimate how R^2_G, A_2, R_H, k_D and c^* vary with excess salt concentration. The measurements were carried out in high-ionic-strength solutions for three excess salt concentrations. Light scattering results show typical good solvent behavior. In particular, at high-ionic strength, the scaling law representing the variation of the diffusion coefficient with polymer concentration in semidilute regime is similar to neutral polymers in good solvent.

The increase of the virial coefficients A_2 and k_D with decreased ionic strength is characteristic of the expansion of the polyelectrolyte chain and electrostatic repulsion interactions. With decreasing ionic strength, the hydrodynamic radius and the radius of gyration become larger due to the expansion of the polyelectrolyte coil. The models for polyelectrolytes and semirigid polyelectrolytes were introduced to analyze and to calculate the variation of the size of the polyion. Good agreement was found between the theoretical and experimental data. The cross-over concentration c^* separating the dilute from the semidilute regime was determined using viscosity, and static and dynamic light scattering. Good agreement was found between different methods used in this study.

References

[1] M. Rinaudo, G. Pavlov and J. Desbrière (1999). *Polymer*, **40**, 7029.
[2] T. Odijk (1977). *J. Polym. Sci., Polym. Phys.*, **15**, 477.
[3] J. Skolnick and M. Fixman (1977). *Macromolecules*, **10**, 944.
[4] M. Fixman (1982). *J. Chem. Phys.*, **76**(12), 6346.
[5] M. Le Bret (1982). *J. Chem. Phys.*, **76**(12), 6243.
[6] G. S. Manning (1969). *J. Chem. Phys.*, **51**, 924.
[7] H. Z. Cummins and E. R. Pike (1974). *Photon Correlation and Light Beating Spectroscopy* (Plenum Press: New York).
[8] D. E. Koppel (1972). *J. Chem. Phys.*, **57**, 4814.
[9] S. W. Provencher (1985). *Makromol. Chem.*, **82**, 632.
[10] P. G. de Gennes (1979). *Scaling Concepts in Polymer Physics* (Cornell University Press: Ithaca).
[11] T. Alfrey (1947). *J. Coll. Sci.*, **2**, 99.
[12] M. Schmidt and W. Burchard (1981). *Macromolecules*, **14**, 210.
[13] A. Z. Akcasu, M. Benmouna and S. Alkhafaji (1981). *Macromolecules*, **14**, 147.

[14] J. J. Tanahatoe and M. E. Kuil (1997). *Macromolecules*, **30**, 6102.
[15] H. Benoît and P. Doty (1953). *J. Phys. Chem.*, **57**, 958.
[16] H. Yamakawa (1972). *Modern Theory of Polymer Solutions* (Harper and Row: NYC.).
[17] C. E. Reed and W. F. Reed (1990). *J. Chem. Phys.*, **92**, 6916.
[18] S. K. Gupta and W. C. Forsman (1972). *Macromolecules*, **5**, 779.
[19] T. Odijk and A. C. Houwaart (1978). *J. Polym. Sci. Phys. Ed.*, **16**, 627.
[20] M. Fixman and J. Skolnick (1978). *Macromolecules*, **11**, 863.
[21] W. F. Reed, S. Ghosh, G. Medjhadi and J. François (1991). *Macromolecules*, **24**, 6189.
[22] R. M. Peitzsch, M. Burt and W. F. Reed (1992). *Macromolecules*, **25**, 806.
[23] M. Rinaudo, I. Roure and M. Milas (1999). *Int. J. Polym. Anal. Charact.*, **5**, 277.
[24] J. M. Schurr and K. S. Schmitz (1986). *Annu. Rev. Phys. Chem.*, **37**, 271.
[25] N. Imai and M. Mandel (1982). *Macromolecules*, **15**, 1562.
[26] M. Mandel (1987). *Physica*, **147A**, 99.
[27] R. G. Smits, M. E. Kuil and M. Mandel (1993). *Macromolecules*, **26**, 6808.